Fault Detection and Isolation and Fault Tolerant Control of Wind Turbines Using Set-Valued Observers

Casau, Pedro; Rosa, Paulo Andre Nobre; Tabatabaeipour, Seyed Mojtaba; Silvestre, Carlos

Published in:
8th IFAC Symposium on Fault Detection, Supervision and Safety of Technical Processes

DOI (link to publication from Publisher):
10.3182/20120829-3-MX-2028.00214

Publication date:
2012

Document Version
Publisher's PDF, also known as Version of record

8th IFAC Symposium on Fault Detection,
Supervision and Safety of Technical Processes (SAFEPROCESS)
August 29-31, 2012. Mexico City, Mexico

Fault Detection and Isolation and Fault Tolerant Control of Wind Turbines using Set-Valued Observers

P. Casau, * **P. Rosa,** * **S. M. Tabatabaeipour,** **
C. Silvestre *,***

* *Institute for Systems and Robotics - Instituto Superior Técnico, Av. Rovisco Pais, 1, 1049-001 Lisboa, Portugal (e-mails: {pcasau,prosa,cjs}@isr.ist.utl.pt).*
** *Aalborg University, 9220 Aalborg East, Denmark (e-mail: smt@es.aau.dk).*
*** *Faculty for Science and Technology, University of Macau, Taipa, Macau.*

Abstract: Research on wind turbine Operations & Maintenance (O&M) procedures is critical to the expansion of Wind Energy Conversion systems (WEC). In order to reduce O&M costs and increase the lifespan of the turbine, we study the application of Set-Valued Observers (SVO) to the problem of Fault Detection and Isolation (FDI) and Fault Tolerant Control (FTC) of wind turbines, by taking advantage of the recent advances in SVO theory for model invalidation. A simple wind turbine model is presented along with possible faulty scenarios. The FDI algorithm is built on top of the described model, taking into account process disturbances, uncertainty and sensor noise. The FTC strategy takes advantage of the proposed FDI algorithm, enabling the controller reconfiguration shortly after fault events. Additionally, a robust controller is designed so as to increase the wind turbine's performance during low severity faults. Finally, the FDI algorithm is assessed within a publicly available benchmark model, using Monte-Carlo simulation runs.

1. INTRODUCTION

As public awareness to climate change rises, so does the political and private support to the research of new and more environmentally friendly energy sources, in order to reduce greenhouse gases emissions and overall dependence on fossil fuels. Wind energy conversion (WEC) systems play a major role in the struggle to achieve this goal IEA [2011], WWEA [2011], EWEA [2010], Blanco [2009].

Both CMS and FDS employ state-of-the-art monitoring technologies which provide early warnings in the presence of any malfunction. The implementation of these systems yields several advantages, including: a) avoidance of premature breakdown; b) reduction of maintenance costs; c) remote diagnosis; d) improvement of the capacity factor [1], and; e) support for future wind turbine development Hameed et al. [2009]. However, wind farm monitoring still relies on the decisions of a human operator or on practical knowledge from experienced staff. New CMS and FDS tend to be driven towards fully autonomous operation. Some algorithms which are still under intensive research include: a) parameter estimation methods; b) observer-based methods; c) knowledge base expert systems, and; d) learning agents Hameed et al. [2009]. The work reported in this article discusses the application of a novel observer-based algorithm to Fault Detection and Isolation (FDI) of wind turbines. Alternative set-membership approaches to FDI can be found in Combastel and Raka [2009], Ingimundarson et al. [2009] and references therein.

[1] The capacity factor is the ratio between the actual power delivered during a time period and the power that would have been produced had the generator been operating at its full capacity Burton et al. [2001].

Standard observer-based approaches to fault detection are discussed in Patton and Chen [1997]. These methods require the computation of thresholds which indicate whether a fault has occurred or not. In this paper, we propose a novel strategy to perform FDI in wind turbines, making use of Set-Valued Observers (SVOs) (c.f. Shamma and Tu [1999]). According to the proposed algorithm, whenever a prespecified bound on the sensors noise or the process disturbances is violated, the SVO may provide the empty set as the set-valued state estimate, which is symptomatic of a faulty behavior. The main advantage of the proposed method is that the nature of the sensor noise or process disturbances need not be specified but only their bounds. This is of particular importance for FDI algorithms of wind turbines, as the wind turbulence and its interaction with the rotor are complex and hard to model. A major problem of any FDI method lies on the distinguishability between any two process models. This problem is addressed in Rosa et al. [2011] within the scope of SVOs and will also be discussed in this paper.

The implementation of FDI strategies in wind turbines yields several advantages. Not only does it provide information about the turbine's health and maintenance requirements, but it also provides a trigger for controller reconfiguration. In this paper we discuss the implementation of two distinct strategies for Fault Tolerant Control (FTC) of wind turbines: a passive approach and an active approach. The passive approach relies on the design of a controller that is robust to plant uncertainties and inherently increases the performance of the wind turbine in the presence of process disturbances. However, this passive solution must be complemented with an active solution which mainly consists on the combination of the proposed FDI algorithm with a logic switching mechanism that either ignores readings from a faulty sensor, selects

a different controller or even completely shuts down the turbine operation in the event of a high severity fault.

This paper is organized as follows. In Section 2 we present the model of the wind turbines followed by the possible fault scenarios in Section 3. We describe the application of the FDI and FTC algorithm using SVOs to wind turbines in Sections 4 and 5, respectively, along with simulation results from the benchmark model in Section 6, see Odgaard et al. [2009].

2. THE WIND TURBINE MODEL

This paper focuses on the application of Fault Detection and Isolation algorithms using Set-Valued Observers (SVOs) to horizontal axis wind turbines. Any of these turbines is composed of several parts, including: the tower, the blades, the rotor hub, the drive train, the converter, several sensors, yaw drive, controller, among others. Since our main goal is the evaluation of the proposed algorithm within the simulation environment described in Odgaard et al. [2009] we will take advantage of the models for the rotor hub, the drive train and the converter dynamics, therein presented.

Figure 1 depicts the connection between the parts of the turbine considered in the dynamic model provided in Odgaard et al. [2009], where v_w is the wind speed, β_i denotes the i-th blade pitch angle [2] , τ_r represents the rotor torque, ω_r represents the rotor speed, τ_g represents the generator torque, ω_g represents the generator rotational speed and P_g represents the power output. The controller provides pitch control and generator torque control using redundant measurements from the blades pitch ($\beta_{i_{mj}}$ for $i \in \{1,2,3\}$ and $j \in \{1,2\}$), the rotor speed $\omega_{r_{mj}}$, generator speed $\omega_{g_{mj}}$, generator torque τ_{g_m} and output power P_{g_m}. These measurements are provided to the FDI algorithm along with the anemometer's readings. Each component has redundant sensors, allowing the control system to reconfigure itself when a sensor fault occurs, in order to ignore the measurements coming from the faulty sensor.

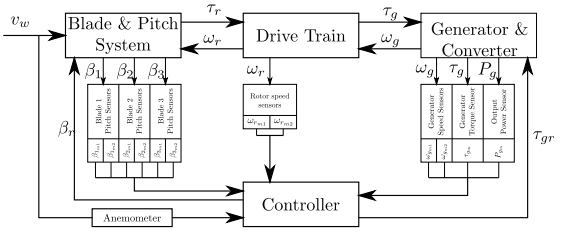

Fig. 1. Simplified wind turbine system illustrating the connections between each of its components.

Aerodynamic Model A fairly detailed description of the wind turbine aerodynamic model can be found in Burton et al. [2001]. A very important characteristic of the aerodynamic performance of the wind turbine is its power coefficient, C_p, which is the ratio between the power delivered to the shaft P_{shaft} and the total wind power P_{wind}, given by $P_{wind} = \rho A v_w^3/2$, where $A = \pi R^2$ is the rotor disk area, R denotes the rotor radius, ρ denotes the atmospheric density and v_w denotes the wind velocity. From the power delivered to the low speed shaft, we compute the rotor torque, which is given by

$$\tau_r = \frac{P_{shaft}}{\omega_r} = \frac{1}{2}\rho\pi R^3 C_q(\lambda,\beta)v_w^2, \qquad (1)$$

[2] The blade pitch is the angle between the zero lift line of the blade and the rotor disk plane

where ω_r is the rotor's rotational speed, $\lambda = \omega_r R/v_w$ is the tip speed ratio, β denotes the blade pitch and $C_q(\lambda,\beta) = C_p(\lambda,\beta)/\lambda$ is the torque coefficient. This coefficient can be computed from experimental data or from theoretical models described throughout the literature (see e.g. Burton et al. [2001]).

Equation (1) implicitly assumes that the pitch angle is the same for every blade. However this is not true since each blade can control its pitch independently. Nevertheless, the rotor torque can be approximated by

$$\tau_r \approx \sum_{i=1}^{3} \frac{\rho\pi R^3 C_q(\lambda,\beta_i)v_w^2}{6},$$

as long as the pitch angle is approximately the same for all three blades of a wind turbine, see Odgaard et al. [2009].

Hydraulic Pitch System Model The blade's pitch system is usually a hydraulic mechanical system which does not instantaneously respond to reference pitch commands β_r and does not necessarily have zero static error. In order to account for these shortcomings and to increase performance/robustness there exists a inner control loop. The transfer function of this system can be approximated by

$$\frac{\beta_i(s)}{\beta_r(s)} = \frac{\omega_n^2}{s^2 + 2\xi\omega_n s + \omega_n^2},$$

where ω_n is the nominal system's bandwidth and ξ is the nominal system's damping Odgaard et al. [2009].

Drive Train Model The drive train is the mechanical linkage that connects the rotor to the generator. The overall system can be modeled as the connection of two masses over a shaft with finite torsion stiffness, subject to torsion damping and imperfect transmission efficiency. A gearbox amplifies the rotor's speed so as to fit the requirements of a given generator. Moreover, either the rotor and the generator are subject to speed damping due to friction.

The differential equations which model the dynamics of the system are given by

$$\begin{bmatrix}\dot{\omega_r}\\ \omega_g \\ \theta_\Delta\end{bmatrix} = \mathbf{A}_{dt}\begin{bmatrix}\omega_r\\ \omega_g \\ \theta_\Delta\end{bmatrix} + \mathbf{B}_{dt}\begin{bmatrix}\tau_r\\ \tau_g\end{bmatrix}$$

with $\mathbf{A}_{dt}$ and $\mathbf{B}_{dt}$ as in Odgaard et al. [2009]. The reader is referred to Heier [1998] for further details regarding the drive train modeling.

Generator and Converter Model The most common generator on a variable speed wind turbine is the Doubly Fed Induction Generator, whose dynamics can be modeled by a first order transfer function

$$\frac{\tau_g}{\tau_{gr}} = \frac{\alpha_{gc}}{s + \alpha_{gc}},$$

where τ_g is the generator torque, τ_{gr} is the generator reference torque and α_{gc} is a given parameter (see Odgaard et al. [2009]). The output power, P_g, depends on the generator speed and torque, as given by $P_g = \eta_g\omega_g\tau_g$, where η_g is the efficiency of the generator.

Controller Regions Wind turbines typically have four operating regions, depending on the wind conditions: region #1 – wind turbine inoperative due to low wind conditions; region #2 – the generator torque is adjusted so as to produce optimal power output; region #3 – turbine operation at rated power using aerodynamic brakes; region #4 – the wind turbine operation is halted using hydraulic

brakes in order to prevent structural damage due to high wind speed.

3. FAULT SCENARIOS

In any mechanical or electrical system, there is an infinite number of possible fault situations. However, to keep the problem to a tractable level, we restrict our analysis to the faults listed in Table 1. The possible faults include sensor errors, as well as changes in the dynamics of the hydraulic systems and each of these faults constitutes a threat to the turbine's operation. A level of severity is attributed to each fault, depending on the amount of damage that may result from it.

In general, sensor faults have low severity levels due to sensor redundancy and because the controllers are typically able to reconfigure themselves in order to ignore any faulty sensor readings. The faults in the dynamics have higher severity levels, as they usually cause slow control actions, which may, in turn, induce permanent damage to the wind turbine. Therefore, depending on these severity levels, each fault has different FDI requirements. Thus, the implemented algorithm must: be able to detect each fault within the maximum time for detection specified in Table 1; keep false detections separate by at least 100000 sampling periods; turn off a false detection after 3 sampling periods; be robust to disturbances; be able to respond rapidly to failures, by either stopping the wind turbine operation or by reconfiguring the controller structure.

4. FDI OF WIND TURBINES

The subject of FDI algorithms using SVOs are described in the companion paper by Rosa et al. [2011], therefore we will only address it briefly in this section. The first task in the implementation of the proposed FDI algorithm is to describe the wind turbine dynamics through an LPV model of the form

$$\begin{aligned}\mathbf{x}[n+1] &= \mathbf{A}[n]\mathbf{x}[n] + \mathbf{B}[n]\mathbf{u}[n] \\ \mathbf{y}[n+1] &= \mathbf{C}[n+1]\mathbf{x}[n+1] + \mathbf{D}[n+1]\mathbf{u}[n+1].\end{aligned} \tag{3}$$

Combining the wind turbine model described in Section 2 with the LPV structure in (3) we define the state, input and observations vectors

$$\begin{aligned}\mathbf{x} &= \begin{bmatrix}\tau_g & \omega_r & \omega_g & \theta_\Delta & \beta_1 & \beta_2 & \beta_3 & \dot{\beta_1} & \dot{\beta_2} & \dot{\beta_3} & x_f\end{bmatrix}^T \\ \mathbf{u} &= \begin{bmatrix}\tau_{gr} & \tau_r & \beta_r & n_{\tau_g} & n_{\omega_r}^{m_1} & n_{\omega_g}^{m_1} & n_{\omega_r}^{m_2} & n_{\omega_g}^{m_2} & \dots \\ \dots & n_{\beta_1}^{m_1} & n_{\beta_2}^{m_1} & n_{\beta_3}^{m_1} & n_{\beta_1}^{m_2} & n_{\beta_2}^{m_2} & n_{\beta_3}^{m_2} & n_{P_g^m} & u_f\end{bmatrix}^T \\ \mathbf{y} &= \begin{bmatrix}\tau_g & \omega_{r_{m1}} & \omega_{g_{m1}} & \omega_{r_{m2}} & \omega_{g_{m2}} & P_g & \dots \\ \dots & \beta_{1_{m1}} & \beta_{2_{m1}} & \beta_{3_{m1}} & \beta_{1_{m2}} & \beta_{2_{m2}} & \beta_{3_{m2}}\end{bmatrix}^T,\end{aligned}$$

where n_{τ_g} denotes the noise on the generator torque sensor, $n_{\omega_r}^{m_j}$ with $j = 1, 2$ denotes the noise on the j-th rotor speed sensor, $n_{\omega_g}^{m_j}$ with $j = 1, 2$ denotes the noise on the j-th generator speed sensor, $n_{\beta_i}^{m_j}$ with $i = 1, 2, 3$ and $j = 1, 2$ denotes the noise on the j-th sensor of the i-th blade and $n_{P_g^m}$ denotes the noise on the power sensor. Furthermore, a new state variable $x_f \in \mathbb{R}$ and a new input variable $u_f \in \mathbb{R}$ were added to the state-space representation. These two new variables represent the state and the noise input, respectively, of a high pass filter with transfer function

$$H(s) = \frac{\omega_f s}{s + \omega_f},$$

where $\omega_f \in \mathbb{R}$. This high pass filter is applied to the measurements of the first rotor sensor and it allows the determination of the noise that this sensor introduces, eventually enabling the detection of fault number 4.

With these definitions, the continuous-time state-space matrices $\mathbf{A}(t)$, $\mathbf{B}(t)$, $\mathbf{C}(t)$ and $\mathbf{D}(t)$ are given by (2).

When operating in Region #2, it is very difficult to detect fault number 6 because of the lack of distinguishability between the nominal and the faulty system plants. In order to detect this fault, we add a sinusoidal signal $\gamma(t) = 3 + 4\sin(14t)$ [deg] to the pitch angle reference $\beta(t)$ when the controller is operating in region # 2. When properly designed (see Rosa et al. [2011] and the companion paper Rosa et al. [2012]), this signal enhances the distinguishability between the faulty and the nominal system models.

In order to conclude the implementation of the Nominal SVO, it is necessary to define the vectors $\mathbf{b}^+$ and $\mathbf{b}^-$. Since the sensor noise is considered to be Gaussian white noise, the noise vector bounds on the sensor s can be characterized by means of its standard deviation σ_s. The vectors $\mathbf{b}^+$ and $\mathbf{b}^-$ are given by

No.	Fault Location	Cause	Consequence	FDI Time	FTC Action
1	Blade 1 Pitch Sensor 1	Electrical/ mechanical	Fixed value output of 5°	$10T_s$	Switch to Blade 1 Pitch Sensor 2
2	Blade 2 Pitch Sensor 2	Electrical/ mechanical	Decrease in gain factor by 20%	$10T_s$	Switch to Blade 2 Pitch Sensor 1
3	Blade 3 Pitch Sensor 1	Electrical/ mechanical	Fixed value output of 10°	$10T_s$	Switch to Blade 3 Pitch Sensor 2
4	Rotor sensor 1	Electrical/ mechanical	Fixed value output of 1.4 rad/s	$10Ts$	Switch to Rotor sensor 2
5	Rotor sensor 2	Electrical/ mechanical	Increase in gain factor by 10%	$10Ts$	Switch to Rotor sensor 1
5	Generator speed sensor 2	Electrical/ mechanical	Decrease in gain factor by 10%	$10Ts$	Switch to Generator speed sensor 1
6	Blade 2 hydraulic system	Pressure drop in the hydraulic system	Modified dynamic parameters to ω_{n2}	$8T_s$	Stop turbine operation
7	Blade 3 hydraulic system	Air content increase in the oil	Slow change in dynamic parameters to ω_{n3} and ξ_3	$600T_s$	Do nothing (fault handled by robust controller)
8	Generator	Offset in the internal control loop	Torque offset of 2 kN.m	$5T_s$	Do nothing (fault handled by robust controller)
9	Drive train	Increased level of vibrations	Decrease of drive train efficiency by roughly 5%	-	Do nothing (fault handled by robust controller)

Table 1. Fault scenarios implemented in the wind turbine benchmark model Odgaard et al. [2009] and corresponding FTC actions.

$$\mathbf{A}(t) = \left[\begin{array}{c|ccc|c|c} -\alpha_{gc} & & 0_{1\times 3} & & & \\ 0 & & & & & \\ -\frac{1}{J_g} & & \mathbf{A}_{dt} & & 0_{4\times 6} & 0_{4\times 1} \\ 0 & & & & & \\ \hline & & & & \begin{array}{cc} 0_{3\times 3} & I_{3\times 3} \\ -2\omega_n\xi I_{3\times 3} & -\omega_n^2 I_{3\times 3} \end{array} & O_{6\times 1} \\ \multicolumn{4}{c|}{0_{6\times 4}} & & \\ \hline 0 & -\omega_f & 0 & 0 & 0_{1\times 6} & -\omega_f \end{array}\right]$$

$$\mathbf{C}(t) = \left[\begin{array}{cccc|c|c} 1 & 0 & 0 & 0 & & \\ 0 & 1 & 0 & 0 & & \\ 0 & 0 & 1 & 0 & 0_{6\times 6} & 0_{6\times 1} \\ 0 & 1 & 0 & 0 & & \\ 0 & 0 & 1 & 0 & & \\ \eta_{gc}\omega_g(t) & 0 & 0 & 0 & & \\ \hline \multicolumn{4}{c|}{0_{6\times 4}} & \begin{array}{cc} I_{3\times 3} & 0_{3\times 3} \\ I_{3\times 3} & 0_{3\times 3} \end{array} & 0_{6\times 1} \\ \hline 0 & \omega_f & 0 & 0 & 0_{1\times 6} & \omega_f \end{array}\right]$$

$$\mathbf{B}(t) = \left[\begin{array}{ccc|c|c} \alpha_{gc} & 0 & 0 & & \\ 0 & \frac{1}{J_r} & 0 & & \\ 0 & 0 & 0 & & \\ 0 & 0 & 0 & 0_{7\times 12} & 0_{7\times 1} \\ 0 & 0 & 0 & & \\ 0 & 0 & 0 & & \\ 0 & 0 & 0 & & \\ \hline 0 & 0 & \omega_n^2 & & \\ 0 & 0 & \omega_n^2 & 0_{3\times 5} \;\; 0.5\omega_n^2 I_{3\times 3} \;\; -0.5\omega_n^2 I_{3\times 3} \;\; 0_{3\times 1} & 0_{6\times 1} \\ 0 & 0 & \omega_n^2 & & \\ \hline 0 & 0 & 0 & 0\;0\;-\omega_f\;0\;0\;0\;0\;0\;0\;0\;0\;0 & 1 \end{array}\right] \qquad \mathbf{D}(t) = \left[\begin{array}{c|c|c} 0_{3\times 12} & I_{12\times 12} & 0_{12\times 1} \\ \hline 0_{1\times 3} & 0\;0\;\omega_f\;0\;0\;0\;0\;0\;0\;0\;0\;0 & 0 \end{array}\right]. \tag{2}$$

$$\mathbf{b}^+ = \Big[\tau_g[n] \quad \tau_r^+[n] \quad \beta_r[n] \quad k_\sigma\sigma_{\tau_g} \quad \dots$$
$$\dots \quad k_\sigma\sigma_{\omega_r} \quad k_\sigma\sigma_{\omega_g} \quad k_\sigma\sigma_{\omega_r} \quad \dots$$
$$\dots \quad k_\sigma\sigma_{\omega_g} \quad k_\sigma\sigma_\beta\mathbf{1}_{1\times 6} \quad k_\sigma\sigma_{P_g}[n]\Big]^T$$
$$\mathbf{b}^- = \Big[\tau_g[n] \quad \tau_r^+[n] \quad \beta_r[n] \quad -k_\sigma\sigma_{\tau_g} \quad \dots$$
$$\dots \quad -k_\sigma\sigma_{\omega_r} \quad -k_\sigma\sigma_{\omega_g} \quad -k_\sigma\sigma_{\omega_r} \quad \dots$$
$$\dots \quad -k_\sigma\sigma_{\omega_g} \quad -k_\sigma\sigma_\beta\mathbf{1}_{1\times 6} \quad -k_\sigma\sigma_{P_g}[n]\Big]^T$$

where σ_s denotes the standard deviation of the sensor s, τ_r^+ and τ_r^- are suitable upper and lower bounds to the aerodynamic torque τ_r, and the value $k_\sigma = 4.42$ was chosen so as to respect the FDI requirement of 100000 samples between false detections.

The proposed nominal SVO is able to detect fault occurrences. However, it is not able to isolate them. In order to isolate the faults listed in Table 1 we will resort to [Rosa, 2011, Architecture 2]. Therefore, the design of fault tolerant SVOs is required. The design of SVOs which are tolerant to a single fault enables the isolation of a fault as long as every other SVO fails. Moreover, the design of a *Global SVO*, which is tolerant to every considered fault, enables the faulty SVOs to recover. This is particularly important whenever a false detection occurs. The design of fault tolerant SVOs is described in Rosa [2011] and it essentially revolves around different ways to add conservatism to the SVOs.

The state machine model which regulates the FDI algorithm is presented in Figure 2. In short, the operation of this state machine abides by the following set of rules, where t_d denotes the time since fault detected mode was last entered and t_i denotes time since fault isolated mode was last entered: i) Switching from nominal mode to fault detected mode is triggered whenever any SVO returns the empty set as the set-valued state estimate; ii) Switching from fault detected mode to nominal mode occurs in the event of a false detection, i.e. if $t - t_d \geq T_f$, where $T_f > 0$ is a design parameter; iii) Switching from fault detected mode to fault isolated mode occurs whenever the k-th SVO and the Global SVO are non-faulty (this corresponds to the isolation of fault number k); iv) Switching from fault isolated mode to nominal mode occurs if all SVOs are non-faulty for $t - t_i \geq T_i$, where T_i is a design parameter; v) Switching from fault isolated mode to fault detected mode occurs if some SVOs are faulty for $t - t_i \geq T_i$. Notice that T_f must be greater than the maximum time for isolation of any of the faults, otherwise the algorithm issues a recovery from a false detection when it should be waiting for fault isolation. On the other hand, $T_f \leq 3T_s$ in order to comply with the requirements. For the algorithm we propose this is not achieved, as we will see in Section 6, because it takes longer than three sampling times from detection until isolation for some of the faults. The parameter T_i can be tuned to each particular fault so as to avoid false recoveries.

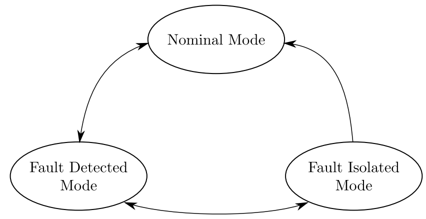

Fig. 2. FDI state machine.

5. FTC OF WIND TURBINES

Under faulty scenarios, the use of controllers designed for the nominal operation of the plant can lead to severe performance deterioration and, ultimately, to instability and damage of the wind turbine. As previously stated, the approach suggested in this paper uses a mixed solution to the FTC problem of wind turbines. In this section, therefore, we start by designing a robust controller in order to guarantee closed-loop stability and enhanced performance both in normal operation and in the event of a failure. Indeed, if such a fault occurs, this controller will prevent additional damages to the wind turbine, until the FDI system is capable of detecting and isolating the fault, so that the control system can be reconfigured.

The FTC system for wind turbines described in this section is built upon the results presented in Section 4, since the fault detection and identification is the mechanism that triggers the controller reconfiguration. The FTC encompasses two different approaches: Active - The inputs of the system are excited whenever the information obtained from the measured outputs is not sufficient to detect and isolate the faults. At the same time, these measured outputs are continuously scanned and the FDI algorithm searches for fault events. On such events, the controller is reconfigured according to the details provided in Table 1; Passive - Robust controllers are used, in order to account for parametric uncertainties and process disturbances, and allowing the operation of the wind turbine under low severity faulty scenarios.

5.1 Robust Controller Design

The synthesis of controllers that are robust against different types of uncertainties and time-variations on the

dynamics of the plant has deserved considerable attention over the last decades. The interested reader is referred, for instance, to Skogestad and Postlethwaite [2005], Zhou et al. [1996]. Among the many alternatives in the literature, the technique adopted in this paper is referred to as *mixed-μ* synthesis. A mixed-μ controller is an approximation of the optimal controller in the $\mathcal{L}_2$-induced norm sense, from the exogenous inputs to the performance outputs. Despite the sub-optimality of the solution, these controllers are capable of handling different types of uncertainties, namely complex and parametric uncertainties, resorting to the so-called D,G-K iterations – see Young [June 1994] and references therein.

The wind turbine model previously described was used to the synthesis of the mixed-μ controller, with the additional requirement that the closed-loop system remains stable not only under nominal operation, but also in the presence of faults #6 or #7. Therefore, the dynamics of the blades can be described by

$$\begin{bmatrix}\dot{\beta}\\ \dot{\beta}_a\end{bmatrix} = \begin{bmatrix}0 & 1\\ -\omega_n^2 & -2\zeta\omega_n\end{bmatrix}\begin{bmatrix}\beta\\ \beta_a\end{bmatrix} + \begin{bmatrix}0\\ \omega_n^2\end{bmatrix}\beta_r, \qquad (4)$$

where $\omega_n \in [3.42,\ 11.11]$ rad/s and $\zeta \in [0.25,\ 0.9]$. In this methodology, the selection of the dynamic weights is key in order to ensure proper disturbance rejection at the desired frequencies, as well as to avoid high-frequency command signals to be sent to the control inputs. The approach adopted in this paper is fully described in Fekri et al. [2006], and consists in optimizing a given performance criterion. In this particular case, the design diagram used is depicted in Fig. 3, and the weights were selected as follows:

$$W_{u1} = \frac{0.1(s+1)}{s+100},\ W_{u2} = 0.01,\ W_{d1} = \frac{1}{s+1},$$
$$W_{d2} = \frac{0.001}{s+1},\ W_{d3} = \frac{3}{s+30},\ W_{p1} = A_{p1}\frac{0.1}{s+0.1},$$
$$W_{p2} = A_{p2}\frac{50}{s+50}.$$

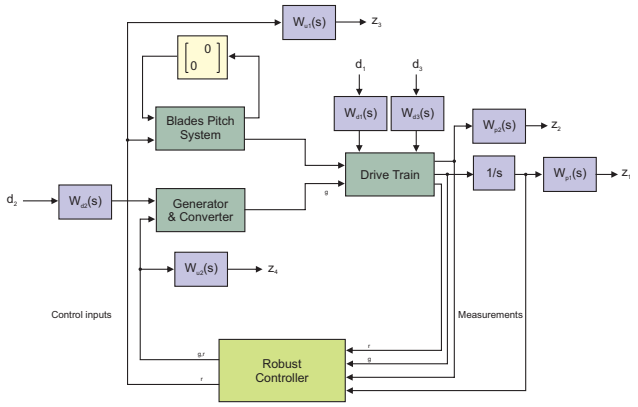

Fig. 3. Block-diagram for robust controller synthesis of the wind turbine model.

By maximizing the values of A_{p1} and A_{p2}, while guaranteeing a value of μ smaller than one, we obtain: $A_{p1} = 0.1$ and $A_{p2} = 0.005$.

5.2 Scheduling of the Controllers

The mixed-μ design method briefly described above assumes that the linearized model of the wind turbine is an accurate description of the corresponding dynamics. Nevertheless, a linearization is typically performed around a trimming point. This trimming point, in turn, depends solely on the wind speed, since nominal values of all state variables can be obtained as functions of v_w. Hence, as soon as the linearized model, for a particular value of v_w, no longer describes the dynamics of the wind turbine, a controller designed for the current value of the wind speed should be connected to the loop. For further details, the reader is referred to Rugh and Shamma [2000].

In this paper, three different regions are considered for the wind speed, as they lead to linearized models of the wind turbine that accurately cover the typical behaviors of this system, see Bianchi et al. [2006]. Indeed, the first model was obtained by linearizing the model of the dynamics of the wind turbine around $\bar{v}_w^1 = 13$ m/s, while the second one considered $\bar{v}_w^2 = 15$ m/s, and the third one assumed $\bar{v}_w = 17$ m/s.

Based on the estimated wind speed, the appropriate mixed-μ controller is connected to the loop. For the sake of simplicity, the controller is selected by the trimming wind speed which is closest (in the Euclidean norm sense) to the estimated wind speed. Thus, the following regions are obtained: $\Omega_1 = [0, 14]$ m/s, $\Omega_2 =]14, 16]$ m/s, and $\Omega_3 =]16, v_w^{\max}[$ m/s,

where $v_w^{\max}$ is such that the wind turbine is shut down if the estimated wind speed exceeds that value. The scheduling of the controllers uses the so-called *D-Methodology* – see Kaminer et al. [1995] – which endows the system with auto-trimming and anti-windup capabilities and it also ensures continuous feedback signals, even if the controller gain swithces due to the scheduling of the controllers.

6. SIMULATION RESULTS

The fault detection capability of the proposed algorithm was tested within the benchmark model discussed in Odgaard et al. [2009] and all the model parameters can be found in the given reference.

Monte-carlo simulations were executed in order to assess the fault detection performance of the proposed algorithm. Since the overall simulation is highly time consuming we have restricted the simulation time to a region around the fault occurence. If the fault is not detected until 7 seconds after its occurrence then we consider that the algorithm is not able to detect it [3]. This is the case for fault numbers 4 and 9, thus we did not include them in 2, where we summarize the simulation results. From the analysis of Table 2 one may check all but faults number 1, 2 are detected within the fault detection requirements listed in Table 1.

This analysis reveals a shortcoming of the FDI strategy that we propose: since we are only assuming that the noise is bounded and we do not assume any other knowledge on the noise inflicted upon the system, then if the fixed values that the sensors exhibit in faults 1 and 4 are not far enough from the values of the corresponding state variable, then the fault may not be detected within reasonable time.

The analysis of Table 2 also reveals that there is a performance decrease with respect to the fault detection results for faults number 2 and 6 and that, most of the time, the remaining faults are always isolated in the same sampling time they are detected. The poor fault isolation performance of fault number 2 arises from the lack of distinguishability between the fault tolerant SVO for fault 2 and the fault tolerant SVO for fault number 6.

We conclude that, overall, the the proposed FDI algorithm has a good performance but must be complemented with other methods if the whole set of faults is to be detected. A main hindrance in the performance of the proposed FDI algorithm is its demand for computational resources. If

[3] Recall that the least demanding FDI specification requires a fault detection within 6 seconds (Fault 7).

additional computation power was avaiable then the set-valued estimates provided by the algorithm would be more accurate and, consequently, the overall performance would improve.

Fault no.	Median Detection Time [s]	Max. Detection Time [s]	Median Isolation Time [s]	Max. Isolation Time [s]
1	0.26	0.26	0.26	0.27
2	1.19	6.55	6.585	6.67
3	0.01	0.01	0.01	0.01
5	0.01	0.01	0.01	0.01
6	0.01	0.01	0.035	0.07
7	3.855	3.93	3.855	3.93
8	0.01	0.01	0.01	0.02

Table 2. Fault detection and isolation simulations results for 20 simulation runs.

In Figure 4 we compare the turbine operation with and without fault tolerant control. In this example, we considered that the PID and the robust controllers were used in a faulty scenario. In particular, we assumed that $\zeta = 0.9$ and $\omega_n = 3.42$ in (4). In terms of tracking of ω_r, the deterioration of performance of the PID when compared to the controller designed in this section is apparent from Fig. 4. Moreover, the RMS of the blades' pitch angles is reduced by 20% due to the use of a robust controller.

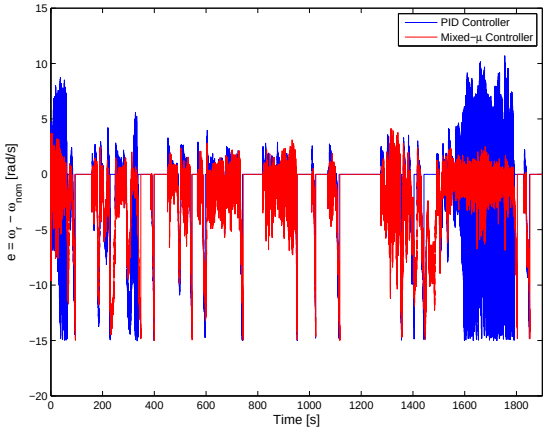

Fig. 4. Tracking error of the rotor speed, ω_r, using the PID and the mixed-μ controller.

7. CONCLUSIONS & FUTURE WORK

In this paper we presented a Fault Detection and Isolation (FDI) algorithm based on set-valued observers. The algorithm was tested within a benchmark model of a wind turbine using Monte-Carlo simulation runs. A Fault Tolerant Controller (FTC) was built on top of the proposed FDI algorithm, enabling the recofiguration of the controller structure during faults. Additionally, a robust controller was designed in order to increase the operational availability of the wind turbine and its performance with respect to standard control techniques. Future work includes the study of novel techniques which may decrease the computational expense of the proposed algorithm without compromising its reliability.

REFERENCES

Fernando D. Bianchi, Hernn de Battista, and Ricardo J. Mantz. *Wind Turbine Control Systems: Principles, Modelling and Gain Scheduling Design (Advances in Industrial Control)*. Springer, 2006.

Mara Isabel Blanco. The economics of wind energy. *Renewable and Sustainable Energy Reviews*, 13(6-7):1372 – 1382, 2009. ISSN 1364-0321. doi: 10.1016/j.rser.2008.09.004.

T. Burton, David Sharpe, Nick Jenkins, and Ervin Bossanyi. *Wind Energy Handbook*. John Wiley & Sons, 2001.

C. Combastel and S.A. Raka. A set-membership fault detection test with guaranteed robustness to parametric uncertainties in continuous time linear dynamical systems. In *Fault Detection, Supervision and Safety of Technical Processes*, pages 1192–1197, 2009.

EWEA. The wind initiative - wind power research and development for the next ten years, 2010.

S. Fekri, M. Athans, and A. Pascoal. Robust multiple model adaptive control (RMMAC): A case study. *Int. Journal of Adaptive Control and Signal Processing*, 21(1):1–30, 2006.

Z. Hameed, Y.S. Hong, Y.M. Cho, S.H. Ahn, and C.K. Song. Condition monitoring and fault detection of wind turbines and related algorithms: A review. *Renewable and Sustainable Energy Reviews*, 13(1):1 – 39, 2009. ISSN 1364-0321. doi: 10.1016/j.rser.2007.05.008.

Siegfried Heier. *Grid Integration of Wind Energy Conversion Systems*. John Wiley & Sons, 1998.

IEA. Technology roadmap - wind energy, 2011.

A. Ingimundarson, J.M. Bravo, V. Puig, T. Alamo, and P. Guerra. Robust fault detection using zonotope-based set-membership consistency test. *International Journal of Adaptive Control and Signal Processing*, 23(4):311–330, 2009.

Isaac Kaminer, Antonio M. Pascoal, Pramod P. Khargonekar, and Edward E. Coleman. A velocity algorithm for the implementation of gain-scheduled controllers. *Automatica*, 31(8):1185 – 1191, 1995.

Peter Fogh Odgaard, Jakob Stoustrup, and Michel Kinnaert. Fault tolerant control of wind turbines - a benchmark model. In *7th Symposium on Fault Detection, Supervision and Safety of Technical Processes*, 2009.

R. J. Patton and J. Chen. Observer-based fault detection and isolation: Robustness and applications. *Control Engineering Practice*, 5(5):671 – 682, 1997. ISSN 0967-0661. doi: 10.1016/S0967-0661(97)00049-X.

P. Rosa, P. Casau, C. Silvestre, S. Tabatabaeipour, and J. Stoustrup. A set-valued approach to fdi and ftc: Theory and implementation issues. In *IFAC SAFEPROCESS*, 2012.

Paulo Rosa. *Multiple-Model Adaptive Control of Uncertain LPV Systems*. PhD thesis, Instituto Superior Técnico, 2011.

Paulo Rosa, Carlos Silvestre, Jeff S. Shamma, and Michael Athans. On the distinguishability of discrete time invariant dynamic systems. In *In Proceedings of the 50th IEEE Conference on Decision and Control*, 2011.

WJ Rugh and J.S. Shamma. A survey of research on gain-scheduling. *Automatica*, 36(10):1401–1425, 2000.

J.S. Shamma and Kuang-Yang Tu. Set-valued observers and optimal disturbance rejection. *Automatic Control, IEEE Transactions on*, 44(2):253 –264, feb 1999. ISSN 0018-9286. doi: 10.1109/9.746252.

S. Skogestad and I. Postlethwaite. *Multivariable Feedback Control: Analysis and Design, 2nd Ed.* John Wiley and Sons, 2005.

WWEA. World wind energy report 2010, 2011.

P.M. Young. Controller design with mixed uncertainties. In *American Control Conference*, pages 2333–2337, Baltimore, Maryland, June 1994.

K. Zhou, J.C. Doyle, and K. Glover. *Robust Optimal Control*. Prentice Hall, 1996.